Tetrahedron 66 (2010) 9396–9400

Contents lists available at ScienceDirect

Tetrahedron

journal homepage: www.elsevier.com/locate/tet

Fluorescence properties of novel 6-butyl-2,3-dicyano-7-methyl-6*H*-1,4-diazepine styryl dyes containing ethyleneglycol units

Masaki Matsui *, Kazuna Noguchi, Yasuhiro Kubota, Kazumasa Funabiki

Department of Materials Science and Technology, Faculty of Engineering, Gifu University, 1-1 Yanagido, Gifu 501-1193, Japan

ARTICLE INFO

Article history:
Received 21 July 2010
Received in revised form 28 September 2010
Accepted 28 September 2010
Available online 21 October 2010

Keywords:
Fluorescence
Ethyleneglycol unit
Styryl dye
Diazepine
Aggregation induced emission enhancement

ABSTRACT

The fluorescence properties of novel 6-butyl-2,3-dicyano-7-methyl-6*H*-1,4-diazepine styryl dyes having mono-, di-, tri-, and tetra(ethyleneglycol) units were examined. The mono(ethylenglycol) derivative was solid at room temperature, whereas the di-, tri-, and tetra(ethylenglycol) derivatives were oily. The monoethyleneglycol derivative showed weak aggregation-induced emission enhancement with fluorescence maximum at 649 nm, which comes from J-aggregates. The fluorescence of oily di-, tri-, and tetra (ethyleneglycol) derivatives in neat form was very weak. No aggregation-induced emission enhancement was observed for the oily derivatives.

1. Introduction

2,3-Dicyano-7-methyl-6*H*-1,4-diazepine styryl dyes are unique compounds having non-planar carbon atom at the 6-position. These dyes show red fluorescence in the solid state.[1] In a series of our study on the fluorescence properties of diazepine styryl dyes, we suspected that, when ethyleneglycol (EG) units are introduced into the molecule, these dyes can be soluble in water and the solid-state fluorescence intensity may be enhanced due to bulky EG units. However, we found that these EG derivatives were scarcely soluble in water. Interestingly, the di-, tri-, and tetraEG derivatives were oily at room temperature, whereas the monoEG derivative was solid. To our knowledge, no clear differences between the fluorescence properties in the solid and neat form as well as between the fluorescence from suspension and emulsion have been reported so far. We serendipitously found the different fluorescence behavior of oily derivatives from solid ones. Meanwhile, aggregation-induced emission enhancement (AIEE) has been reported not only for siloles[2] and tetraarylethylenes[3] but also for dyes, such as BODIPY,[4] 4-dicyanomethylene-2,6-distyryl-4*H*-pyrans,[5] polyenes,[6] and Sudan II.[7] Therefore, it is of significance to find new AIEE dyes. We could find that suspended monoEG derivative showed weak AIEE. We report herein the fluorescence properties of 6-butyl-2,3-dicyano-7-methyl-6*H*-1,4-diazepine styryl dyes having mono-, di-, tri-, and tetraEG units.

2. Results and discussion

2.1. Synthesis of 6-butyl-2,3-dicyano-7-methyl-6*H*-1,4-diazepine styryl dyes 3

6-Butyl-2,3-dicyano-7-methyl-6*H*-1,4-diazepine styryl dyes **3** were synthesized as shown in Scheme 1. 6-Butyl-2,3-dicyano-5,7-dimethyl-6*H*-1,4-diazepine (**1**) was allowed to react with 4-formylanilines containing EG units **2** in the presence of piperidine to provide **3**.

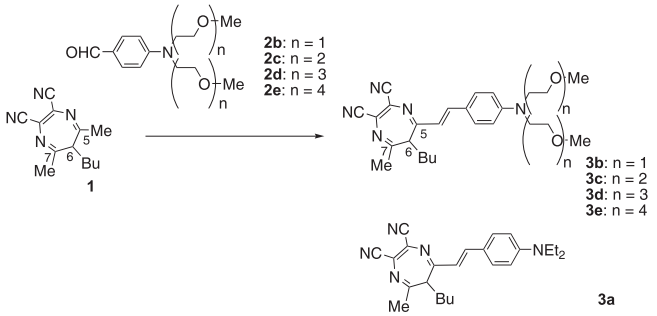

Scheme 1. Reagents and conditions: **1** (1.1 equiv), **2** (1.0 equiv), piperidine, THF, reflux, 24 h.

* Corresponding author. E-mail address: matsuim@gifu-u.ac.jp (M. Matsui).

0040-4020/$ – see front matter © 2010 Elsevier Ltd. All rights reserved.
doi:10.1016/j.tet.2010.09.103

2.2. Solubility of 6-butyl-2,3-dicyano-7-methyl-6*H*-1,4-diazepine styryl dyes

The solubility of **3** is shown in Table 1. These compounds were scarcely soluble in water at 25 °C. The solubility of **3** in methanol was higher with increasing number of EG units. Compound **3e** was most soluble in methanol, there being 5.3 g dm^{-3}, followed by in ethanol, 1-propanol, 2-propanol, 1-butanol, and EG.

Table 1
Physical properties of 6-butyl-2,3-dicyano-7-methyl-6*H*-1,4-diazepine styryl dyes **3**

Compd	Solubility in methanol[a]	In ethanol[b]			Solid state		
	g dm^{-3} (mmol dm^{-3})	λ_{max} (ε)/nm	F_{max}/nm	Φ_f[c]	λ_{ex}[d] (ε)/nm	F_{max}/nm	Φ_f[c]
3a	0.43 (1.1)	492 (46600)	622	0.04	570	683	0.03
3b	0.50 (1.1)	484 (42400)	623	0.04	590	649	0.06
3c	2.5 (4.7)	481 (40400)	623	0.04	590[e]	681[e]	<0.01[e]
3d	3.9 (6.3)	484 (44300)	627	0.04	590[e]	689[e]	0.01[e]
3e	5.3 (7.4), 5.1 (7.2)[f], 4.8 (6.6)[g] 4.7 (6.6)[h], 4.5 (6.3)[i], 0.51 (0.72)[j]	481 (45600)	621	0.04	573[e]	665[e]	<0.01[e]

[a] Measured at 25 °C.
[b] Measured at the concentration of 1.0×10^{-5} mol dm^{-3} at 25 °C.
[c] Determined by absolute PL quantum yield measurement system C9920-02.
[d] Obtained by measuring diffuse reflectance spectra given in Kubelka–Munk units.
[e] In neat form.
[f] In ethanol.
[g] In 1-propanol.
[h] In 2-propanol.
[i] In 1-butanol.
[j] In ethyleneglycol.

2.3. UV–vis absorption and fluorescence spectra of 6-butyl-2,3-dicyano-7-methyl-6*H*-1,4-diazepine styryl dyes in solution

The UV–vis absorption and fluorescence spectra of **3** in ethanol are shown in Fig. 1. The results are also summarized in Table 1. They showed UV–vis absorption maximum (λ_{max}) at around 485 nm with molar absorption coefficient (ε) in the range of 40,400–46,600. The fluorescence maximum (F_{max}) was observed at around 625 nm with fluorescence quantum yield (Φ_f) 0.04. Thus, no significant differences in the UV–vis absorption and fluorescence spectra were observed among **3a**, **3b**, **3c**, **3d**, and **3e** in ethanol.

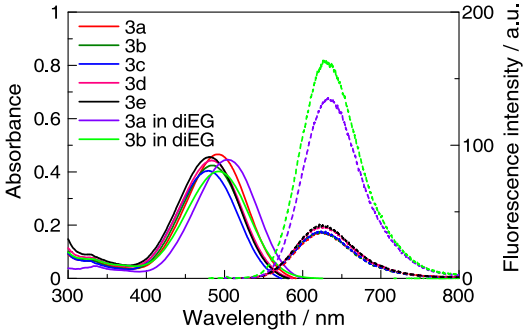

Fig. 1. UV–vis absorption and fluorescence spectra of **3** in ethanol. Measured on 1×10^{-5} mol dm^{-3} of substrate at 25 °C. Solid and dotted lines represent UV–vis absorption and fluorescence spectra, respectively.

2.4. Thermal analysis of oily derivatives

Though compounds **3a** and **3b** were solid, **3c**, **3d**, and **3e** were oily. The DSC of **3c**, **3d**, and **3e** are shown in Fig. 2. They showed endothermic peak at −0.7, −25.4, and −30.6 °C, respectively. These peaks correspond to the melting point. When **3d** was chilled from room temperature to −120 °C, the exothermic peak was observed at around −30 °C. Then, by heating this sample, endothermic peak was observed at around −30 °C as shown in Fig. S1 in the Supplementary data.

2.5. Fluorescence spectra of 6-butyl-2,3-dicyano-7-methyl-6*H*-1,4-diazepine styryl dyes in solid and neat form

The fluorescence spectra of **3a** and **3b** in the solid state and those of **3c**, **3d**, and **3e** in neat form are depicted in Fig. 3. Compounds **3a** and **3b** showed F_{max} at 683 and 649 nm, respectively, there being more bathochromic than those in ethanol (622 and 623 nm) due to intermolecular interactions in the solid state.

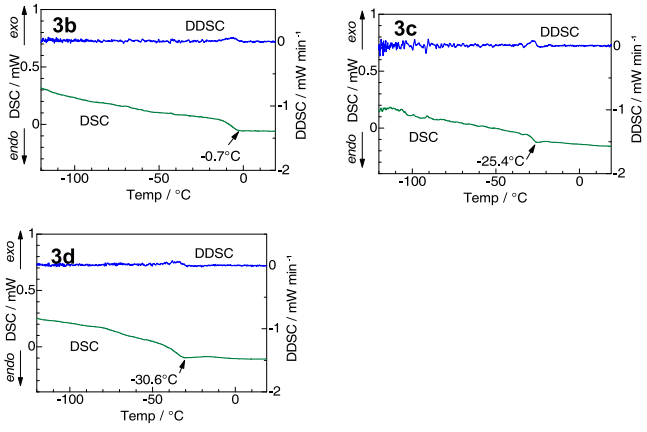

Fig. 2. DSC of **3c**, **3d**, and **3e**. A sample was chilled to −150 °C for 20 min, then heated to room temperature at the rate of 10 °C min^{-1}. DDSC means derivative differential scanning calorimetry.

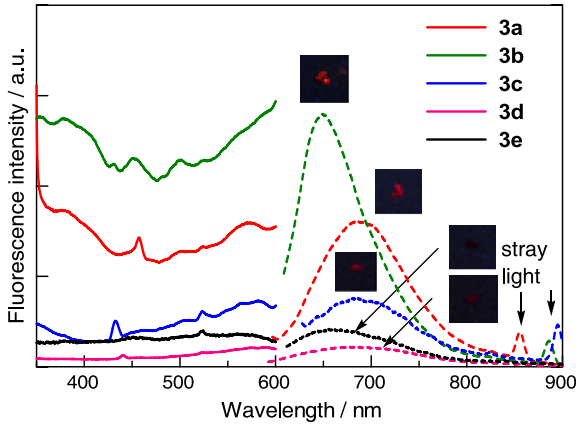

Fig. 3. Excitation and fluorescence spectra of **3**. Compounds **3a** and **3b** were measured in the solid state. Compounds **3c**, **3d**, and **3e** were measured in neat form.

Interestingly, the F_{max} of **3b** was most hypsochromic among **3a**, **3b**, **3c**, **3d**, and **3e**. Furthermore, the Φ_f of **3b** in the solid state (0.06) was larger than that in ethanol (0.04), suggesting AIEE.

In Fig. 1, no significant differences in the UV–vis absorption spectra of **3a** and **3b** between in ethanol (viscosity: 1.06 cp at 25 °C) and in diEG (30 cp at 25 °C)[8] were observed. Nevertheless, the fluorescence of **3a** in diEG was significantly more intense than that in ethanol, indicating that the inhibition of free rotation in the phenylene ring could exhibit stronger fluorescence. Furthermore, the fluorescence of **3b** in diEG was more intense than that of **3a**. These results indicate that the AIEE of **3b** could come from not only free rotation inhibition of the phenylene ring but also that of ether linkages in the solid state.

The F_{max} of **3c**, **3d**, and **3e** in neat form was observed in the range of 665–689 nm. Their Φ_f was very low (<0.01). The fluorescence intensity in neat form and solid state is affected by molecular packing and rigidity of the fluorophore. It is clear that the melting point of oily derivatives is lower than the solid derivatives. The probability of the internal conversion from the first excited singlet state to the ground state of oily compounds can be larger than that of solid ones. Therefore, usually, the fluorescence intensity of oily derivative is less than that of solid ones.

The reflection, fluorescence, and excitation spectra of **3b** in potassium bromide are shown in Fig. 4. The reflection band became broad at higher concentration, indicating the formation of aggregates. The F_{max} showed slight bathochromic shift from 620 to 649 nm with increasing concentration of **3b**. The fluorescence intensity gradually increased with increasing concentration of **3b** from 0.01 to 10% of **3b**. At 100% **3b**, the intensity slightly decreased. The excitation maximum at around 520 nm caused bathochromic shift at higher concentration. These results suggest that the fluorescence of **3b** in the solid state results from J-aggregates.

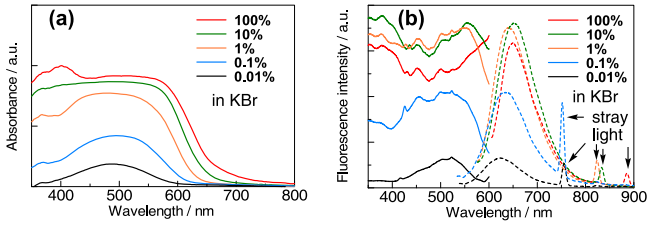

Fig. 4. (a) Reflection and (b) excitation and fluorescence spectra of **3b** in potassium bromide. Solid and dotted lines in Fig 4b represent excitation and fluorescence spectra, respectively.

2.6. AIEE test for 3b and 3e

In the course of this study, we found that compounds **3** were scarcely soluble in water. When the aqueous mixture of **3** was filtered through the membrane filter (0.45 μm), the substrate was recovered on the filter surface. This could be attributed to the low content ratio of hydrophilic EG units in the molecule. Fig. 5 shows color change of **3b** and **3e** in methanol/water mixed solvent upon green laser irradiation. Both compounds **3b** and **3e** show red emission in methanol, indicating that these compounds are completely soluble in methanol. By adding water, green light scattering gradually increased. At 95% water content, only green light scattering was observed. This result indicates that they were not soluble in the mixed solvent even at low concentration of **3b** 1.0×10^{-5} mol dm^{-3}. At 95% water content, compound **3b** showed stronger scattering than **3e**. Solid **3b** and oily **3e** could form suspension and emulsion in the mixed solvent, respectively. Stronger scattering of laser could occur on the surface of suspension than that on emulsion.

Next, the differences of fluorescence behavior between **3b** and **3e** in methanol/water mixed solvent were examined. The UV–vis

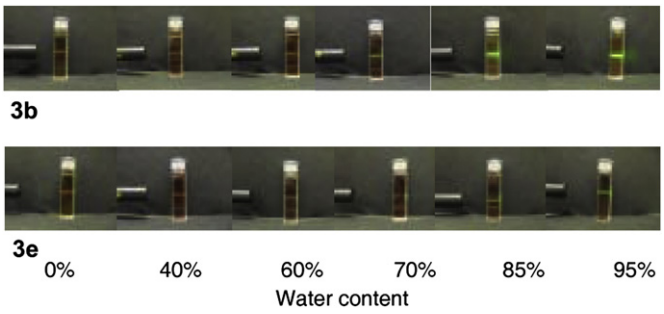

Fig. 5. Picture of **3b** and **3e** in methanol/water mixed solvent upon green laser irradiation. Measured on 1×10^{-5} mol dm^{-3} of substrate.

absorption, fluorescence, and excitation spectra of **3b** are shown in Fig. 6. Fig. 6a and b depict that the UV–vis absorption band becomes broad by adding water. The amount of dissolved **3b** in methanol/water mixed solvent gradually decreased from 0 to 50% water content, and then by adding more water, the shoulder peak at around 570 nm gradually increased, indicating the formation of J-aggregates. Fig. 6c and d exhibit that the F_{max} caused slight bathochromic shift by adding water. The excitation spectra also became broad by adding water, which is similar to the UV–vis absorption spectra. Fig. 6e depicts that the fluorescence intensity gradually decreased by adding water up to 50%, then slightly increased up to water content 95%.

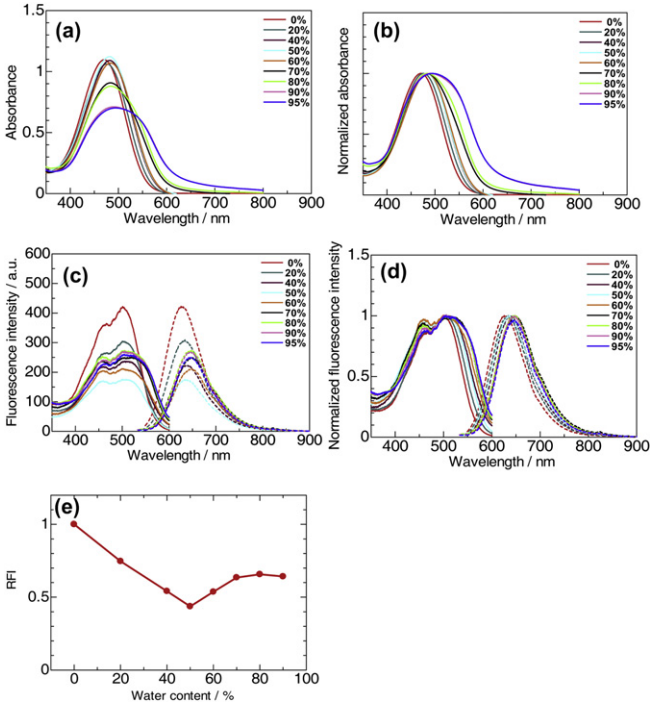

Fig. 6. (a) UV–vis absorption of **3b**, (b) normalized UV–vis absorption spectra of **3b**, (c) excitation and fluorescence spectra of **3b**, (d) normalized excitation and fluorescence spectra of **3b**, and (e) relationship between fluorescence intensity and water content of **3b** in methanol/water mixed solvent. Measured on 1×10^{-5} mol dm^{-3} of substrate at 25 °C. Solid and dotted lines in Fig. 6c and d represent excitation and fluorescence spectra, respectively.

The UV–vis absorption and fluorescence spectra of **3b** and **3e** in various solvents are shown in Figs. S2 and S3 in the Supplementary data, respectively. The fluorescence intensity of **3b** and **3e** increased as polar was the solvent. Therefore, a small amount of **3b** dissolved in methanol/water mixed solvent may enhance the emission.

However, though the fluorescence intensity of **3e** also increased in polar solvent, this compound did not show increased fluorescence intensity in methanol/water mixed solvent as indicated in Fig. 7e. Furthermore, the increase in the fluorescence intensity of **3b** is proportional to the formation of J-aggregates whose Φ_f in the solid state is larger than that in methanol as shown in Fig. 6a, b, and e. These results indicate that the increased fluorescence intensity in methanol/water mixed solvent results from AIEE and not from solvent effects.

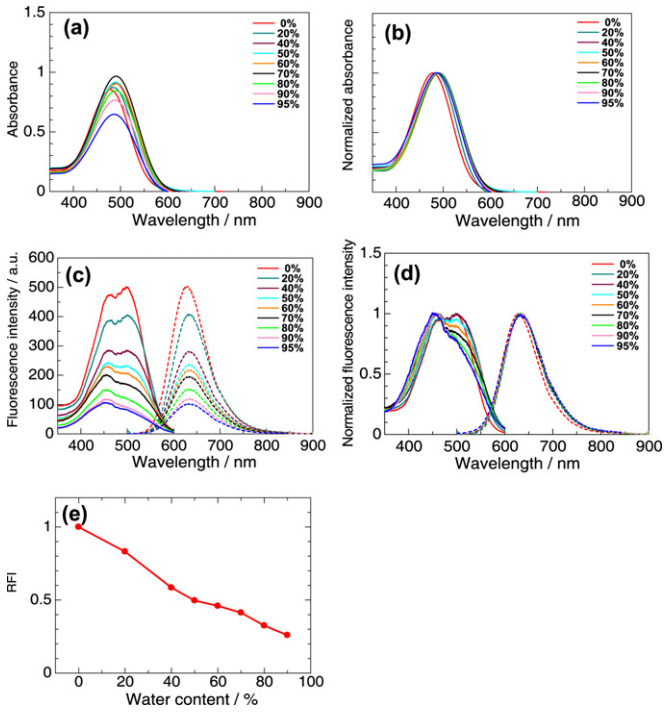

Fig. 7. (a) UV–vis absorption spectra of **3e**, (b) normalized UV–vis absorption spectra of **3e**, (c) excitation and fluorescence spectra of **3e**, (d) normalized excitation and fluorescence spectra of **3e**, and (e) relationship between fluorescence intensity and water content of **3e** in methanol/water mixed solvent. Measured on 2.5×10^{-5} mol dm^{-3} of substrate at 25 °C. Solid and dotted lines in Fig. 7c and d represent excitation and fluorescence spectra, respectively.

Siloles and tetraarylethylenes can show AIEE because of inhibition of C-aromatic bond rotation.[2a] In the case of **3b**, the C-aromatic and C–O bonds rotation could be inhibited in the solid state to show AIEE. As compound **3b** is soluble in 100% methanol, the emission from the solution is observed. When water is added to the methanol solution, compound **3b** forms suspension, and at the same time, the amount of **3b** dissolved in methanol decreases. The fluorescence intensity of the solvent depends on the balance between the amount of dissolved **3b** and that of suspended **3b**. The amount of **3b** dissolved in methanol decreases until 50% water content as shown in Fig. 6a. Then, by adding more water, the amount of J-aggregates gradually increases as depicted in Fig. 6b. The relationship between the size of produced dye particle and water content is shown in Fig. S4. Interestingly, the size of the aggregates in 80% water content was bigger than that in 50% water content to enhance the fluorescence intensity. However, the difference of Φ_f of **3b** between in the solid state and solution is much smaller than that of siloles and tetraarylethylenes. Therefore, the increase in the fluorescence intensity of **3b** by adding water is not so drastic as siloles and tetraarylethylenes.

The UV–vis absorption and fluorescence spectra of **3e** in methanol/water mixed solvent are shown in Fig. 7. Fig. 7a and b indicate that oily **3e** showed no drastic aggregation formation even in 95% water content. Fig. 7c and d depict that no drastic bathochromic shift in F_{max} was observed in the mixed solvent. As no remarkable bathochromic shift in the excitation spectra was observed for **3e**, in comparison with those of **3b**, the fluorescence could mainly comes from the monomer form. The fluorescence intensity of **3e** gradually decreased by adding water as shown in Fig. 7e.

Thus, solid compound **3b** formed suspension in methanol/water mixed solvent to exhibit weak AIEE. Meanwhile, oily compound **3e** formed emulsion in the mixed solvent not to show AIEE.

2.7. X-ray crystallography of 3b

The X-ray crystallography of **3b** was performed. The result is indicated in Fig. 8. Molecules form a pair of head-to-tail dimer, the intermolecular distance being 3.65 Å. Weak π/π-interactions are observed between the pair of molecules. The dimers are packed in parallel. Weak CH/π interactions are observed between adjacent molecules A and D. The transition moment of the dimer is 1.23 D by the DFT calculations (B3LYP/6-31G(d,p)) (Supplementary data Fig. S1). The slip angle is calculated to be 12.5°. It is reported that when the slip angle is smaller than 54.7°, the UV–vis absorption band could cause bathochromic shift.[9] The enhancement of solid-state fluorescence by J-aggregates has been reported.[10] Thus, compound **3b** could form J-aggregates in the solid state to show bathochromic and more intense fluorescence in the solid state than in solution.

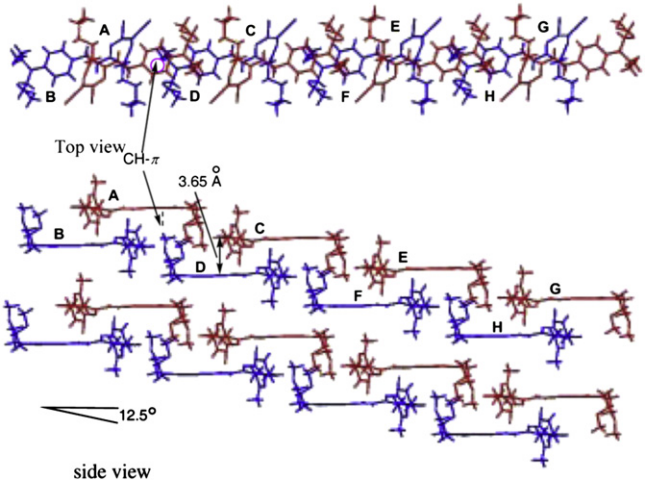

Fig. 8. X-ray crystallography of **3b**.

3. Conclusion

The fluorescence properties of non-planar and novel 6-butyl-2,3-dicyano-7-methyl-6*H*-1,4-diazepine styryl dyes having mono-, di-, tri-, and tetraEG units were examined. They are scarcely soluble in water. The tetraEG derivative showed the highest solubility in methanol. Among the EG derivatives, the monoEG derivative **3b** is solid at room temperature. This compound showed F_{max} at 649 nm with Φ_f 0.06, which is larger than that in ethanol. This compound formed suspension in methanol/water mixed solvent and exhibited weak AIEE due to the inhibition of free rotation of phenylene and ether moieties. This fluorescence could come from J-aggregates. Meanwhile, the di-, tri-, and tetraEG derivatives are oily at room temperature. Their fluorescence was very weak (Φ_f<0.01) in neat from. They formed emulsion in methanol/water mixed solvent and showed no AIEE.

4. Experimental

4.1. General

Melting points were measured with a Yanaco MP-13 micro-melting-point apparatus. NMR spectra were obtained by a JEOL ECX 400P spectrometer. MS spectra were measured with a JEOL MStation 700 spectrometer. UV–vis absorption, reflection, and fluorescence spectra were taken on Hitachi U-3500, U-4000, and F-4500 spectrophotometers, respectively. Fluorescence quantum yields were measured by a Hamamatsu Photonics Absolute PL Quantum Yield Measurement System C9920-02. 6-Butyl-2,3-dicyano-5,7-dimethyl-6*H*-1,4-diazepine (**1**),[1] 4-formylanilines,[5] and 6-butyl-2,3-dicyano-5-[4-(diethylamino)styryl]-7-methyl-6*H*-1,4-diazepine (**3a**)[1] were synthesized as described in the literature.

*4.1.1. Synthesis of 6-butyl-2,3-dicyano-7-methyl-6H-1,4-diazepine styryl dyes **3**.* To a THF solution of 6-butyl-2,3-dicyano-5,7-dimethyl-6*H*-1,4-diazepine (**1**, 251 mg, 1.1 mmol) and 4-(dialkylamino)benzaldehydes **2** (1 mmol) was added piperidine (5 drops). The mixture was refluxed for 24 h. After the reaction was completed, the solvent was removed in vacuo. The product was purified by column chromatography (SiO_2, **3b**/CH_2Cl_2/MeOH=100:1, **3c**/CH_2Cl_2/MeOH=90:1, **3d**/CH_2Cl_2/MeOH=80:1, **3e**/CH_2Cl_2/MeOH=60:1).

*4.1.2. 6-Butyl-2,3-dicyano-5-{4-[bis(2-methoxyethyl)amino]styryl}-7-methyl-6H-1,4-diazepine (**3b**).* Yield 20%; mp 136–138 °C; IR (KBr) ν 2223 cm^{-1}; ^1H NMR ($CDCl_3$) δ=1.00 (t, J=6.9 Hz, 3H), 1.26 (m, 1H), 1.42–1.53 (m, 4H), 2.04 (s, 3H), 2.17–2.37 (m, 2H), 3.35 (s, 6H), 3.56 (t, J=5.4 Hz, 4H), 3.64 (t, J=5.4 Hz, 4H), 6.33 (d, J=15.1 Hz, 1H), 6.71 (d, J=9.2 Hz, 2H), 7.41 (d, J=9.2 Hz, 2H), 7.67 (d, J=15.1 Hz, 1H); ^{13}C NMR ($CDCl_3$) δ=13.9, 21.6, 22.6, 26.5, 30.0, 51.0, 57.4, 59.1, 70.0, 110.7, 111.8, 115.5, 115.6, 119.7, 119.7, 122.6, 130.8, 147.7, 150.4, 150.7, 154.2; EIMS (70 eV) m/z (rel intensity) 447 (M^+, 14), 402 (100); EIHRMS m/z 447.2680, calcd for $C_{26}H_{33}N_5O_2$, 447.2634.

*4.1.3. 6-Butyl-2,3-dicyano-5-(4-{bis[2-(2-methoxyethoxy)ethyl]amino}styryl)-7-methyl-6H-1,4-diazepine (**3c**).* Yield 15%; −0.7 °C; IR (KBr) ν 2222 cm^{-1}; ^1H NMR ($CDCl_3$) δ=1.00 (t, J=6.9 Hz, 3H), 1.25–1.27 (m, 1H), 1.42–1.54 (m, 4H), 2.05 (s, 3H), 2.17–2.34 (m, 2H), 3.38 (s, 6H), 3.52 (t, J=5.8 and 5.8 Hz, 4H), 3.60 (t, J=5.8, 5.8 Hz, 4H), 3.65 (m, 8H), 6.33 (d, J=15.1 Hz, 1H), 6.71 (d, J=9.0 Hz, 2H), 7.40 (d, J=9.0 Hz, 2H), 7.66 (d, J=15.1 Hz, 1H); ^{13}C NMR ($CDCl_3$) δ=13.9, 21.6, 22.6, 26.5, 30.0, 51.0, 57.4, 59.1, 68.3, 70.7, 72.0, 110.7, 111.8, 115.5, 115.6, 119.7, 119.7, 122.6, 130.8, 147.7, 150.4, 150.6, 154.2; EIMS (70 eV) m/z (rel intensity) 535 (M^+, 15), 446 (100); FABHRMS m/z 536.3241 (MH^+), calcd for $C_{30}H_{42}N_5O_4$, 536.3237.

*4.1.4. 6-Butyl-2,3-dicyano-5-[4-(bis{2-[2-(2-methoxyethoxy)ethoxy]ethyl}amino)styryl]-7-methyl-6H-1,4-diazepine (**3d**).* Yield 10%; −25.4 °C; IR (KBr) ν 2222 cm^{-1}; ^1H NMR ($CDCl_3$) δ=1.00 (t, J=6.9 Hz, 3H), 1.26–1.27 (m, 1H), 1.42–1.56 (m, 4H), 2.05 (s, 3H), 2.17–2.38 (m, 2H), 3.37 (s, 6H), 3.53 (t, J=5.5 and 5.5 Hz, 4H), 3.61–3.65 (m, 20H), 6.33 (d, J=15.1 Hz, 1H), 6.71 (d, J=8.7 Hz, 2H), 7.40 (d, J=8.7 Hz, 2H), 7.66 (d, J=15.1 Hz, 1H); ^{13}C NMR ($CDCl_3$) δ=13.9, 21.6, 22.6, 26.5, 30.0, 51.0, 57.4, 59.0, 68.3, 70.5, 70.5, 70.7, 71.9, 110.6, 111.8, 115.5, 115.6, 119.7, 119.7, 122.5, 130.8, 147.7, 150.4, 150.6, 154.2; EIMS (70 eV) m/z (rel intensity) 623 (M^+, 19), 490 (100); EIHRMS m/z 623.3694 (M^+), calcd for $C_{34}H_{49}N_5O_6$, 623.3683.

*4.1.5. 6-Butyl-2,3-dicyano-5-{4-[bis(2,5,8,11-tetraoxa-13-tridecanyl)amino]styryl}-7-methyl-6H-1,4-diazepine (**3e**).* Yield 24%; −30.6 °C; IR (KBr) ν 2222 cm^{-1}; ^1H NMR ($CDCl_3$) δ=1.00 (t, J=7.1 Hz, 3H), 1.26–1.27 (m, 1H), 1.42–1.48 (m, 4H), 2.05 (s, 3H), 2.21–2.38 (m, 2H), 3.38 (s, 6H), 3.54 (t, J=5.7 and 5.7 Hz, 4H), 3.59–3.64 (m, 28H), 6.33 (d, J=15.1 Hz, 1H), 6.71 (d, J=8.9 Hz, 2H), 7.40 (d, J=8.9 Hz, 2H), 7.66 (d, J=15.1 Hz, 1H); ^{13}C NMR ($CDCl_3$) δ=13.9, 21.6, 22.6, 26.5, 30.0, 50.9, 57.4, 59.0, 68.3, 70.5, 70.5, 70.5, 70.5, 70.7, 71.9, 110.6, 111.8, 115.5, 115.6, 119.6, 119.6, 122.5, 130.8, 147.8, 150.4, 150.7, 154.3; EIMS (70 eV) m/z (rel intensity) 711 (M^+, 19), 534 (100); FABHRMS m/z 712.4292 (MH^+), calcd for $C_{38}H_{58}N_5O_8$, 712.4285.

4.2. X-ray crystallography of 3b

Single crystals were obtained by diffusion method using dichloromethane and hexane. The diffraction data were collected by using graphite monochromated Mo Kα radiation (λ=0.71069 Å). The structure was solved by direct methods SIR97 and refined by fill-matrix least-squares calculations. Crystal data for **3b**: $C_{26}H_{33}N_5O_2$, M_w=447.57, triclinic, $P\bar{1}$, Z=2, a=9.342(4), b=10.214(4), c=14.951(6) Å, D_{calcd}=1.227 g cm^{-3}, T=127 K, 9952 reflections were collected, 5489 unique (R_{int}=0.080), 302 parameters, R_1=0.0616, wR_2=0.1322. The crystallographic data (CCDC 782741) have been deposited at the CCDC, 12 Union Road, Cambridge CB2 1EZ, UK.

Supplementary data

Transition dipole moment of **3b** calculated by the TDDFT/B3LYP/6-31G(d,p) level and X-ray crystallographic data of **3b**. Supplementary data associated with this article can be found in the online version at doi:10.1016/j.tet.2010.09.103.

References and notes

1. Horiguchi, E.; Matsumoto, S.; Funabiki, K.; Matsui, M. *Bull. Chem. Soc. Jpn.* **2005**, *78*, 1167.
2. (a) Hong, Y.; Lam, J. W. Y.; Tang, B. Z. *Chem. Commun.* **2009**, 4332, references cited therein; (b) Yuan, W. Z.; Lu, P.; Chen, S.; Lam, J. W. Y.; Wang, Z.; Liu, Y.; Kwok, H. S.; Ma, Y.; Tang, B. Z. *Adv. Mater.* **2010**, *22*, 2159; (c) Luo, J.; Xie, Z.; Lam, J. W. Y.; Cheng, L.; Chen, H.; Qiu, C.; Kwok, H. S.; Zhan, X.; Liu, Y.; Zhu, D.; Tang, B. Z. *Chem. Commun.* **2001**, 1740.
3. Zhao, Z.; Chen, S.; Lam, J. W. Y.; Jim, C. K. W.; Chan, C. Y. K.; Wang, Z.; Lu, P.; Deng, C.; Kwok, H. S.; Ma, Y.; Tang, B. Z. *J. Phys. Chem. C* **2010**, *114*, 7963.
4. Hu, R.; Lager, E.; Aguilar-Aguilar, A.; Liu, J.; Lam, J. W. Y.; Sung, H. H. Y.; Williams, I. D.; Zhong, Y.; Wong, K. S.; Pena-Cabrera, E.; Tang, B. Z. *J. Phys. Chem. C* **2009**, *113*, 15845.
5. Tong, H.; Dong, Y.; Häuûler, M.; Hong, Y.; Lam, J. W. Y.; Sung, H. H.-Y.; Williams, I. D.; Kwok, H. S.; Tang, B. Z. *Chem. Phys. Lett.* **2006**, *428*, 326.
6. Shimizu, M.; Tatsumi, H.; Mochida, K.; Shimono, K.; Hiyama, T. *Chem.—Asian J.* **2009**, *4*, 1289.
7. Yu, H.; Qi, L. *Langmuir* **2009**, *25*, 6781.
8. *Solvent Handbook*; Asahara, T., Tokura, N., Okawara, M., Kumanotani, J., Senoo, M., Eds.; Kohdansya: Tokyo, 1976.
9. Kasha, M.; Rawls, H. R.; El-Bayoumi, M. A. *Pure Appl. Chem.* **1965**, *11*, 371.
10. (a) Kaiser, T. E.; Wang, H.; Stepanenko, V.; Würthner, F. *Angew. Chem., Int. Ed.* **2007**, *46*, 5541; (b) An, B.-K.; Kwon, S.-K.; Jung, S.-D.; Park, S. Y. *J. Am. Chem. Soc.* **2002**, *124*, 14410.